Supplementary note for "Hydrodynamic 2D turbulence and spatial beam condensation in multimode optical fibers"

E. V. Podivilov[1,2], D. S. Kharenko[1,2], V. A. Gonta[1], K. Krupa[3], O. S. Sidelnikov[1,4], S. Turitsyn[1,5], M. P. Fedoruk[1,4], S. A. Babin[1,2], and S. Wabnitz[1,6]

[1] *Novosibirsk State University, Novosibirsk 630090, Russia*

[2] *Institute of Automation and Electrometry SB RAS, 1 ac. Koptyug ave., Novosibirsk 630090, Russia*

[3] *Dipartimento di Ingegneria dell'Informazione, Università di Brescia, Via Branze 38, 25123 Brescia, Italy*

[4] *Institute of Computational Technologies SB RAS, Novosibirsk 630090, Russia*

[5] *Aston Institute of Photonic Technologies, Aston University, Birmingham, B4 7ET, UK and*

[6] *Dipartimento di Ingegneria dell'Informazione, Elettronica e Telecomunicazioni, Sapienza Università di Roma, Via Eudossiana 18, 00184 Roma, Italy*

(Dated: February 15, 2019)

In this note, we present the details of the derivation of a truncated model involving the nonlinear coupling process among three transversal modes only. Let us consider the coupling between modes with $m = 0$, $p = 0, 1, 2$ in Eqs.(1) of the main text, and set $A_p \equiv B_{p,0}$. One obtains

$$\begin{aligned}
2i\frac{dA_0}{d\zeta} &= \left(-D + \frac{p}{\pi}[V_0 I_0 + 2V_{01} I_1 + 2V_{02} I_2]\right) A_0 \\
&\quad + \frac{p}{\pi} V_{02,11} A_1^2 A_2^*, \\
2i\frac{dA_1}{d\zeta} &= \left(-D(2+1)^2 + \frac{p}{\pi}[V_1 I_1 + 2V_{01} I_0 + 2V_{12} I_2]\right) A_1 \\
&\quad + 2\frac{p}{\pi} V_{02,11} A_0 A_2 A_1^*, \\
2i\frac{dA_2}{d\zeta} &= \left(-D(4+1)^2 + \frac{p}{\pi}[V_2 I_2 + 2V_{21} I_1 + 2V_{02} I_0]\right) A_2 \\
&\quad + \frac{p}{\pi} V_{02,11} A_1^2 A_0^*.
\end{aligned} \tag{1}$$

where $A_i \equiv \sqrt{I_i}\exp(i\phi_i)(i = 0, 1, 2)$. We introduced the following overlap integrals

$$V_n = \int_j^\infty du\, L_n^4(u)\exp(-2u),$$

$$V_0 = 1/2, \quad V_1 = 1/4, \quad V_2 = 11/64$$

$$V_{nk} = \int_j^\infty du\, L_n^2(u) L_k^2(u)\exp(-2u),$$

$$V_{01} = 1/4, \quad V_{02} = 3/16, \quad V_{12} = 5/32,$$

$$V_{02,11} = \int_j^\infty du\,(1-u)^2(1-2u+u/2)\exp(-2u) = 1/8$$

The conservation laws $I_0 + I_1 + I_2 = 1$, and $I_0 - I_2 \equiv \alpha = const$ provide us with the relations $I_{0,2}(\zeta) = (1 - \eta \pm \alpha)/2$, where $I_1(\zeta) \equiv \eta < 1$.

From the mode amplitude equations (1), we obtain the evolution equations for the normalized power η of the intermediate transversal mode with $(m = 0, p = 1)$ and the phase $\theta = \phi_0 + \phi_2 - 2\phi_1$ in Hamiltonian form

$$\begin{aligned}
\frac{d\eta}{d\xi} &= \frac{dH}{d\theta}, \\
\frac{d\theta}{d\xi} &= -\frac{dH}{d\eta},
\end{aligned} \tag{2}$$

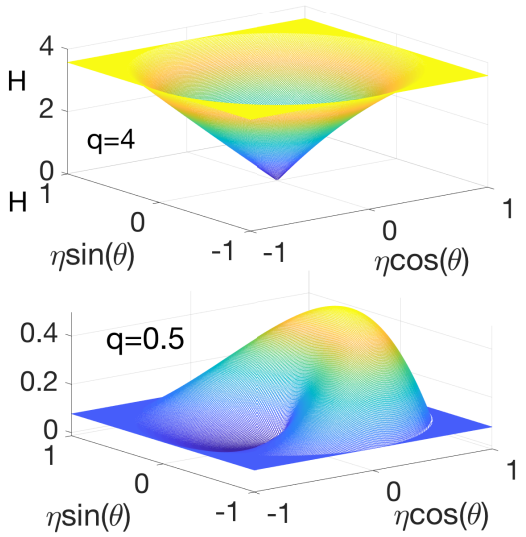

FIG. 1. Hamiltonian H for $q = 4$ and $q = 0.5$, with $\alpha = 0$.

where

$$H = H_T \cos(\theta) + H_S,$$
$$T \equiv -\frac{dH_T}{d\eta}, S \equiv -\frac{dH_S}{d\eta},$$
$$H_T = \eta\sqrt{(1-\eta)^2 - \alpha^2}$$
$$H_S = (q - K_1)\eta + K_2\eta^2$$
$$q = 4D\pi/pV_{02,11} = 32D\pi/p$$
$$\xi = \zeta p V_{02,11}$$
$$K_1 = \frac{\frac{V_0+V_2}{4} + V_{02} - V_{01} - V_{12} + \alpha\left(\frac{V_0-V_2}{4} + V_{01} - V_{12}\right)}{V_{02,11}} =$$
$$-13/32 + \alpha(45/32)$$
$$K_2 = \frac{\frac{V_0+V_2}{4} + V_1 + V_{02} - 2V_{01} - 2V_{12}}{2V_{02,11}} = -53/64$$

We can see that Eqs.2 have the saddle points $\eta_e = 1 - |\alpha|$ and $\eta_e = 0$ at large q. In the linear limit (i.e., for $p \ll D$, or sufficiently large q), the linear wave vector mismatch suppresses the FWM-induced energy exchange between transversal modes.

A bifurcation of the saddle points occurs when new maximum (or minimum) of $H(\theta, \eta)$ appears on the phase diagram. Namely, when $dH/d\theta = 0$, and $dH/d\eta = 0$. The first condition gives us $\theta = 0, \pi$. For $\theta = 0$ (and $\alpha = 0$), we have from the second condition the relation $1 + q - K_1 + 2\eta(K_2 - 1) = 0$. Since $0 < \eta < 1$, one obtains $-1 - (13/32) = K_1 - 1 < q < 1 - 2K_2 + K_1 = 2.25 = q_{1\mathrm{crit}}$. For $q > q_{1\mathrm{crit}}$, there are only rotations on the phase plane around $\eta = 0$ (see Fig. 1, with $q = 4$). The condition $q = q_{1\mathrm{crit}}$ is the threshold of parametric instability. Moreover, for $\theta = \pi$ we have from the second condition the relation $1 - q - K_1 - 2\eta(K_2 + 1) = 0$, and $0.25 = K - 1 - 2K_2 - 1 < q < 1 + K_1 = (19/32) = q_{2\mathrm{crit}}$ For $q < q_{2\mathrm{crit}}$, we have a new extreme point of H.

The bifurcation of the unstable saddle points leads to the generation of new saddle points with coordinate η_e

$$0 = (q - K_1) + 2K_2\eta_e \pm \left(\sqrt{(1-\eta_e)^2 - \alpha} - \eta_e(1-\eta_e)/\sqrt{(1-\eta_e)^2 - \alpha}\right). \quad (3)$$

3D views of the Hamiltonian H in the absence ($q = 4$) and in the presence (q=0.5) of a bifurcation of its saddle points are illustrated in Fig. 1.

The presence of a parametric instability leads to a strong dependence of the spatial mode coupling process upon the input beam launching conditions into the MMF. Fig. 2 shows that in linear conditions (i.e., with $q = 4$) there

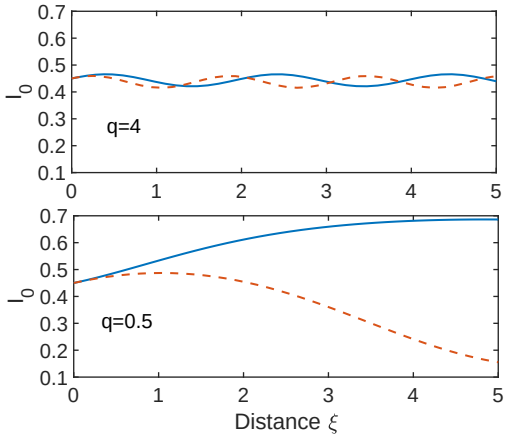

FIG. 2. Evolution of intensity fraction in fundamental mode with either $q = 4$ or $q = 0.5$, and $\alpha = 0.4$, $\eta = 0.5$ (blue solid curves) or $\alpha = 0.1$, $\eta = 0.2$ (dashed orange curves); $\theta(\xi = 0) = 0.35\pi$.

is only a small variation in the intensity oscillation of the fundamental mode as the input conditions are changed. Whereas in the presence of the parametric instability, there is a divergence of the flux of energy in and out of the fundamental mode as the input conditions are slightly modified. In Fig. 2, we have considered two different input conditions, both corresponding to 45% of initial intensity fraction in the fundamental mode. But in the case of the blue solid curves, the highest order mode is excited at the fiber input with only 10% of the total input intensity. This corresponds to the case of an input beam with a relatively small transverse cross-section, so that most of the input intensity is coupled into the fundamental and the intermediate modes. Whereas the orange dashed curves in Fig. 2 correspond to a relatively larger fraction (35%) of input intensity into the high-order transverse mode, as it occurs when the cross-section of the input beam gets larger. The solid blue curve shows that the relative intensity in the fundamental mode grows up to 75% upon propagation into the GRIN MMF. Whereas the orange curve shows that the fundamental mode is initially weakly amplified, but subsequently gets even depleted with distance. Thus we may conclude that self-cleaning should be accompanied by depletion of the intermediate mode, so that energy flows into both the fundamental and the high-order mode.